Lamin-B1 is a senescence-associated biomarker in clear-cell renal cell carcinoma

MELISSA MARIE RADSPIELER[1*], MARIO SCHINDELDECKER[1,2*], PHILIPP STENZEL[1],
SEBASTIAN FÖRSCH[1], KATRIN E. TAGSCHERER[1], ESTHER HERPEL[3,4], MARKUS HOHENFELLNER[5],
GENCAY HATIBOGLU[5], WILFRIED ROTH[1] and STEPHAN MACHER-GOEPPINGER[1,2]

[1]Institute of Pathology, University Medical Center Mainz; [2]Tissue Biobank, University Medical Center Mainz, D-55131 Mainz;
[3]Institute of Pathology, University Hospital Heidelberg; [4]Tissue Bank of The National Center for Tumor Diseases;
[5]Department of Urology, University Hospital Heidelberg, D-69120 Heidelberg, Germany

Abstract. Clear-cell renal cell carcinoma (ccRCC) is a von-Hippel-Lindau gene (*VHL*) associated tumor disease. In addition to activating the hypoxia inducible factor (HIF) dependent oxygen-sensing pathway, *VHL* loss also has an impact on a HIF-independent senescence program which functions as a tumorigenesis barrier. Lamin-B1 is a nuclear intermediate filament protein that exhibits effects on chromatin structure and gene expression and acts as a senescence effector. In the present study, the expression and prognostic relevance of Lamin-B1 in a large cohort of ccRCC patients was examined and the report presents initial functional data on possible therapeutic implications. The expression of Lamin-B1 was measured by immuno-histochemistry using a tissue microarray containing tumor tissue samples from 763 ccRCC patients. Chi-squared tests, Kaplan-Meier curves and Cox regression models were used to investigate the possible association between Lamin-B1 expression, clinical and pathological characteristics and patient survival. High Lamin-B1 expression was associated with poor clinical outcomes and multivariate Cox regression analyses revealed that Lamin-B1 was an independent prognostic factor for cancer-specific survival. Furthermore *in vitro* data suggested that Lamin-B1 acted as a functional downstream senescence effector in RCC cell lines. In conclusion, patients affected by ccRCC with high Lamin-B1 expression exhibit poor prognosis. Lamin-B1 may serve as a tissue-based biomarker for new therapeutic agents targeting therapy-induced senescence.

Introduction

Clear-cell renal cell carcinoma (ccRCC) comprises the majority of malignant tumors in the kidneys (1) and inactivation of the von Hippel-Lindau (VHL) gene is the driving force in ccRCC tumorigenesis. The VHL gene is somatically mutated in up to 80% of sporadic ccRCCs and is causative for the familial cancer syndrome VHL disease that predisposes affected patients to hereditary ccRCC (2). VHL inactivation results in stabilization of hypoxia-inducible factor (HIF), which activates many downstream hypoxia-driven genes, including vascular endothelial growth factor and other genes involved in angiogenesis (3). In addition, there is now a greater appreciation of HIF-independent VHL functions. For instance, VHL loss triggers HIF-independent senescence that is mediated by retinoblastoma protein (Rb) and p400 (4,5). Consistently, senescence occurs in VHL-deficient renal epithelial cells *in vivo* (6). The induction of senescence via the inactivation of tumor-suppressor genes has also been shown for *neurofibromin 1* and *PTEN*, and also via the activation of oncogenes such as *RAS* and *BRAF* (7-10). This mechanism is considered important in order to limit tumor development in mammalian cells (11).

Senescence induced by oncogene activation decreases the expression of Lamin-B1 (LMNB1) (12), a nuclear intermediate filament protein that plays a vital role in DNA replication, the formation of the mitotic spindle, gene transcription and the maintenance of cell proliferation (13). *LMNB1* is an E2F target gene (14) and its down regulation during senescence is mediated by Rb. LMNB1 downregulation has been reported to be a key event following senescence induction and is a trigger of local chromatin changes that result in an impact on global gene expression (15). In addition, silencing LMNB1 expression decreases proliferation and induces premature senescence in human diploid fibroblasts (12). Furthermore, adult-onset autosomal dominant leukodystrophy, a slow progressive neurological disorder characterized by symmetrical widespread myelin loss in the central nervous system, is caused by *LMNB1* duplications resulting in increased gene expression in brain tissue (16).

Correspondence to: Professor Stephan Macher-Goeppinger, Institute of Pathology, University Medical Center Mainz, Langenbeckstrasse 1, D-55131 Mainz, Germany
E-mail: stephan.m-g@unimedizin-mainz.de

*Contributed equally

Little is known about LMNB1 in cancer development and progression. However, LMNB1 expression has been shown to be reduced in gastrointestinal tract neoplasms (17) and lung cancer (18). On the other hand, increased *LMNB1* expression has been observed in prostate (19) and liver cancers (20), and is associated with a poorer clinical outcome in patients with colon (21) and pancreatic cancers (22).

Very little is known about *LMNB1* expression in RCC. Therefore, the present study examined the protein expression of LMNB1 in a large, hospital cohort of patients with RCC with long-term follow-up information to determine if LMNB1 may serve as a novel biomarker in RCC.

Materials and methods

Patients. Tissue samples from 932 patients with primary RCCs treated at the Department of Urology at the University of Heidelberg (Heidelberg, Germany) between 1987 and 2005 were provided by the Tissue Bank of the National Centre for Tumor Diseases Heidelberg (Table I) and used retrospectively in the present study after approval was obtained from the Ethics Committee of the University of Heidelberg. Further details regarding patient evaluation for clinical follow-up have been described previously (23).

Tissue microarray. A tissue microarray containing 932 primary tumors and the corresponding matched normal tissue samples of the 932 patients was created. The tumors were graded according to the 3-tiered nuclear grading system (24) and pathologically staged based on the Tumor-Node-Metastasis classification of 2009 (25).

Immunohistochemistry. Tissues were buffered in 4% formalin overnight in Sakura VIP 2000 (cat. no. 5217031; Sakura Finetek Europe B.V.) at 37°C followed by paraffin-embedding at 60°C. In the next step tissues were cut into 2 μm thick slices using a microtome (Hyrax M55; Carl Zeiss AG). Target retrieval solution (cat. no. K8005; DakoCytomation; Dako; Agilent Technologies, Inc.) was used for antigen retrieval. Briefly, following heat-induced antigen retrieval, which was comprised of initial heating at 94-98°C for 5 min, slides were washed with the kit's washing buffer, rehydrated in descending alcohol series with ethanol concentrations ranging from 50-100% and xylene, and blocked with the kit's blocking solution (Envision Flex Peroxidase-Blocking Reagent) at room temperature for 5 min. Tissue microarray slides were stained with a polyclonal anti-LMNB1 rabbit antiserum (1:1,000) for 30 min at room temperature (Abcam; cat. no. ab16048). For Ki-67, sections were incubated with Flex monoclonal Mouse anti-human Ki-67 Clone MIB-1 (dilution: ready to use solution; EnVision FLEX; Agilent Technologies, Inc.; cat. no. IR626) at room temperature for 20 min according to the manufacturer's protocol.

Staining was performed at room temperature using an automated staining system (Autostainer Plus; Dako; Agilent Technologies, Inc.) in accordance with the manu-facturer's instructions using the following solutions: Flex Envision (cat. no. 8002); Envision Flex DAB+ Chromogen (cat. no. 20052435), Envision Flex Antibody Diluent (cat. no. K8006), Envision Flex Rabbit (Linker; cat. no. K8019) and

Dako Real Hematoxylin (cat. no. S2020). LMNB1 expression was independently scored by light microscopy with magni-fication up to x400 by two of the authors who were blinded to tissue annotations and patient outcomes. For the cell line experiments, digital image analysis was performed.

Cell lines and cell culture experiments. The RCC cell lines, ACHN, 769-P, 786-O and Caki-2 were purchased from American Type Culture Collection. All cell lines were main-tained in RPMI-1640 medium (Thermo Fisher Scientific, Inc.) supplemented with 10% fetal calf serum, 1 mM glutamine, 25 mM glucose and 1% penicillin-streptomycin (all Thermo Fisher Scientific, Inc.) and cultured at 37°C in a 5% CO_2 atmosphere. After recovery from storage in liquid nitrogen, the cells were cultured for no more than 3 months. Senescence was induced using a low dose etoposide (Selleck Chemicals) treatment protocol (769-P cells: 5 μM; ACHN cells: 1 μM; 768-O cells: 2 μM; Caki-2 cells: 20 μM) for 24 h, followed by a 3-5 day recovery phase in normal RPMI culture medium. After this, cell pellets were prepared from exponentially growing cells harvested using accutase (Sigma Aldrich; Merck KGaA; cat. no. A6964). Following centrifugation at 300 x g at 4°C for 5 min, the cells were resuspended, washed in phos-phate-buffered saline and fixed in 4% formalin at 37°C for 15 min (Sigma-Aldrich; Merck KGaA). This was followed by another wash step with PBS and then the cells were transferred into 100% alcohol and precipitated with 30% bovine serum albumin (Carl Roth GmbH & Co. KG). For immunostaining followed by digital image analysis, cell lines were additionally fixed in formalin, paraffin embedded and sectioned into 2 μm slices according to standard protocols that were also used for tissue samples as described previously (5).

Digital image analysis. Prior to image analysis, slides were digitalized using the NanoZoomer-Series Digital slide scanner (Hamamatsu Photonics). Digital image analysis was performed using the HALO® platform from Indica Labs with the CytoNuclear v1.4 module as described previously (26).

The Cancer Genome Atlas (TCGA) data. Disease specific data was generated by the TCGA Research Network (cancerge-nome.nih.gov/) and the cohort used was KIRC-TCGA from 2016-01-28. A self-made R script was utilized to retrieve, process and visualize the relevant data or outcome, respectively.

Statistical analysis. Survival analysis was conducted for 622 patients with a mean survival time of 72.6 months using the functions coxph and survfit from the R package survival (cran.r-project.org/web/packages/survival/index.html; version 2.41-3). LMNB1 protein expression was dichotomized utilizing the Charité Cut-off finder functions to provide a significant distinction between the high and low LMNB1 protein expression levels based on survival outcome (27). Associations between survival times and LMNB1 expres-sion were firstly assessed by log-rank tests and presented as Kaplan-Meier plots. In order to account for the influence of established prognostic factors, hazard ratios (HRs) and 95% confidence intervals (CIs) were adjusted for patient gender and age, tumor extent, lymph node metastasis, distant metastasis, grade of malignancy, and Eastern Cooperative Oncology

Table I. Clinical and pathological features of the study population (n=622).

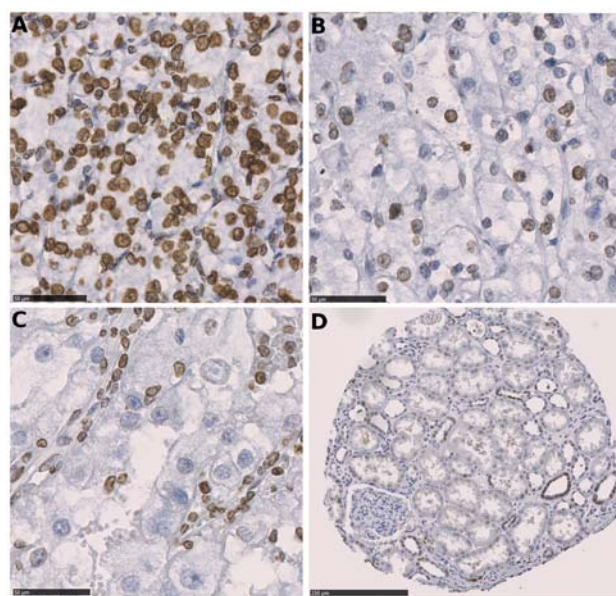| Feature	Total n, (%)
Fuhrman grade	
1	170 (27.3)
2	345 (55.5)
3	107 (17.2)
Tumor grade	
1	334 (53.7)
2	49 (7.9)
3	217 (34.9)
4	22 (3.5)
Local lymph node metastasis	
No	588 (94.5)
Yes	34 (5.5)
Distant metastasis	
No	521 (83.8)
Yes	101 (16.2)
Sex	
Female	249 (40.0)
Male	373 (60.0)
Age at surgery, years	
≤65	353 (56.8)
>65	269 (43.2)
ECOG	
0	381 (61.3)
>0	241 (38.7)

ECOG, Eastern Cooperative Oncology Group.

Figure 1. Immunohistochemical staining of Lamin-B1 expression. (A) Strong positive staining for Lamin-B1 was observed in the majority of ccRCC cells. (B) Moderate positivity was observed in a subset of ccRCC cells. (C) Lamin-B1-negative ccRCC cells; positive endothelial cells and lymphocytes can be seen. Scale bars, 50 μm. (D) Parenchyma of the renal cortex-the majority of the cells of the distal convoluted tubule were positive for Lamin-B1 when compared with only single cells with weak positivity in the proximal convoluted tubule. Scale bar, 250 μm. ccRCC, clear cell renal cell carcinoma.

Group (ECOG) Performance Status in a multiple Cox proportional hazard regression (28). Efron was used as a method for handling tied death times (29) in multivariate analysis of the Cox proportional hazard model (semiparametric and estimation of the HR, CI). Statistical tests were performed using R-Statistical Software (www.rproject.org; version 3.4.3) and R-Studio (version 1.1.383; www.rstudio.com). All plots were created using the following R-packages (cran.r-project. org/): ggplot2 (version 2.2.1.9000), survminer (version 0.4.1), ggpubr (version 0.1.6) and survival. P≤0.05 was considered to indicate a statistically significant difference.

Results

Immunohistochemistry. Immunostaining was performed on tissue microarrays containing tumor and the corresponding normal renal tissues from 932 patients with primary RCCs. The present study is focused on 763 cases with ccRCC, the most common kidney cancer subtype. In total, the cancer tissues of 622 ccRCCs were successfully scored for LMNB1 expression by immunohistochemistry. The remaining cases were excluded from further analyses either due to insufficient tumor tissues, poor tissue preservation or missing patient information. Fig. 1 depicts the immunohistochemical LMNB1 expression in tumor cells; LMNB1 was expressed in distal tubuli, and infrequently and less intensely in proximal tubuli.

Clinical characteristics of the patients. The median time of follow-up was 5.4 years (mean, 6.05 years; maximum, 19.76 years). At the end of the follow-up period, 209 patients had succumbed to RCC; the median follow-up time among these patients was 1.53 years (mean, 2.72 years; maximum, 17.7 years). The clinical and pathological features of the study population are summarized in Table I.

LMNB1 expression and patient prognosis. Based on the Charité Cut-off finder functions (27), 60% positive tumor cells were determined as the cutoff. When tumors were grouped according to LMNB1 expression (>60%, LMNB1-high; ≤60%, LMNB1-low) univariate survival analysis revealed a decrease in cancer-specific survival (HR, 1.63; 95% CI, 1.11-2.41) in patients harboring tumors with high LMNB1 expression compared to tumors with low/no LMNB1 expression. The corresponding Kaplan-Mayer plots are depicted in Fig. 2.

Comparison of LMNB1 expression with clinical and pathological features. No consistent association between LMNB1 expression and differentiation, tumor extent, lymph node metastasis, distant metastasis or patient age was observed (Fig. 3; Table SI).

Multivariate analysis of LMNB1 expression and clinical and pathological features. To further validate the results, multivariate analysis was performed using the Cox proportional
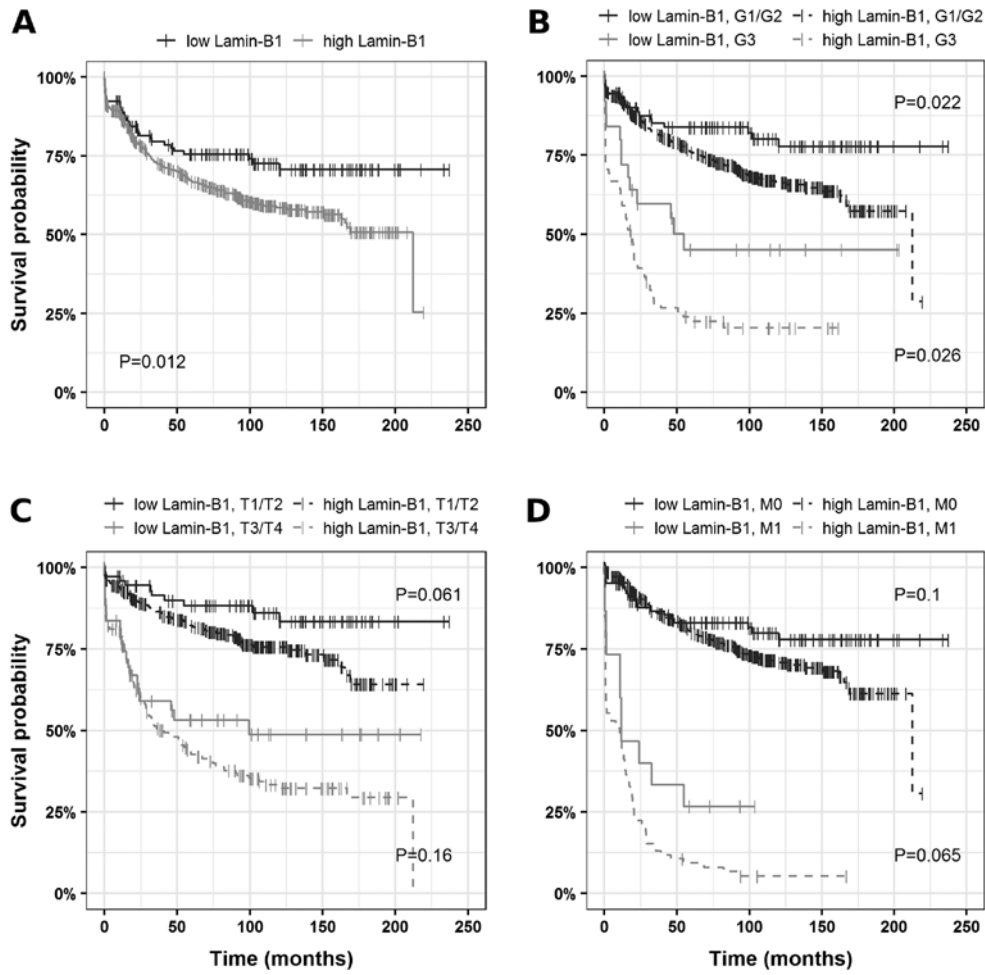
Figure 2. Analysis of cancer-specific survival in ccRCCs. (A) Association between survival times and Lamin-B1 expression presented as Kaplan-Meier plots and subset analysis: (B) high-grade vs. low-grade ccRCCs, (C) advanced vs. restricted tumor extent and (D) localized vs. distant disease. ccRCC, clear cell renal cell carcinoma.
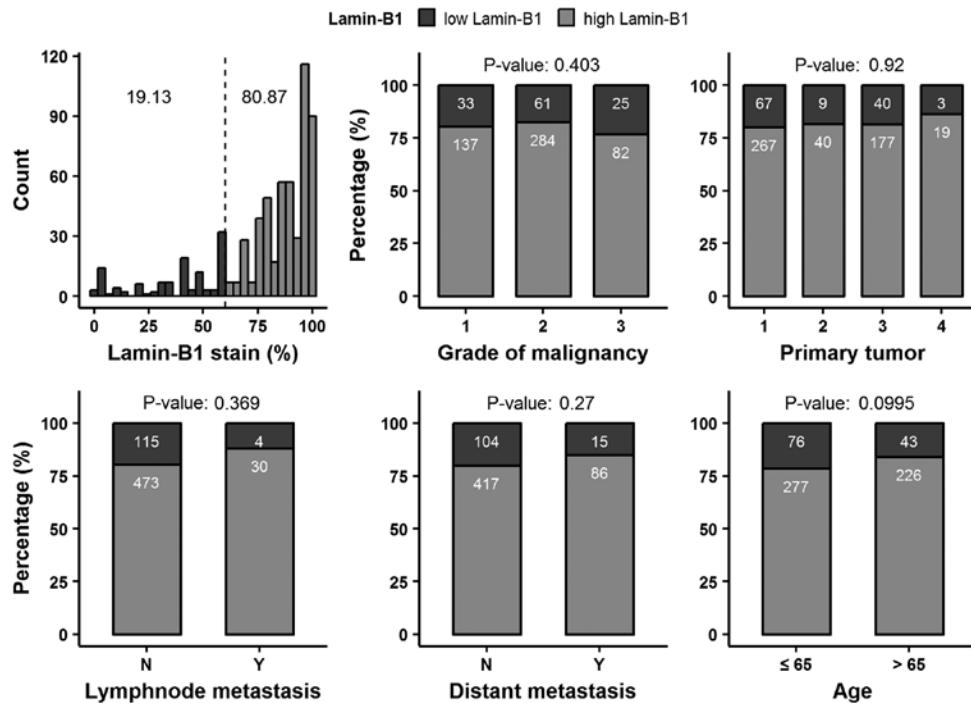

Figure 3. Relative distribution of Lamin-B1 positive cells in clear cell renal cell carcinoma. The dashed line represents the cut-off value (60%) and comparison of Lamin-B1 expression with clinical and pathological features. N, no; Y, yes.
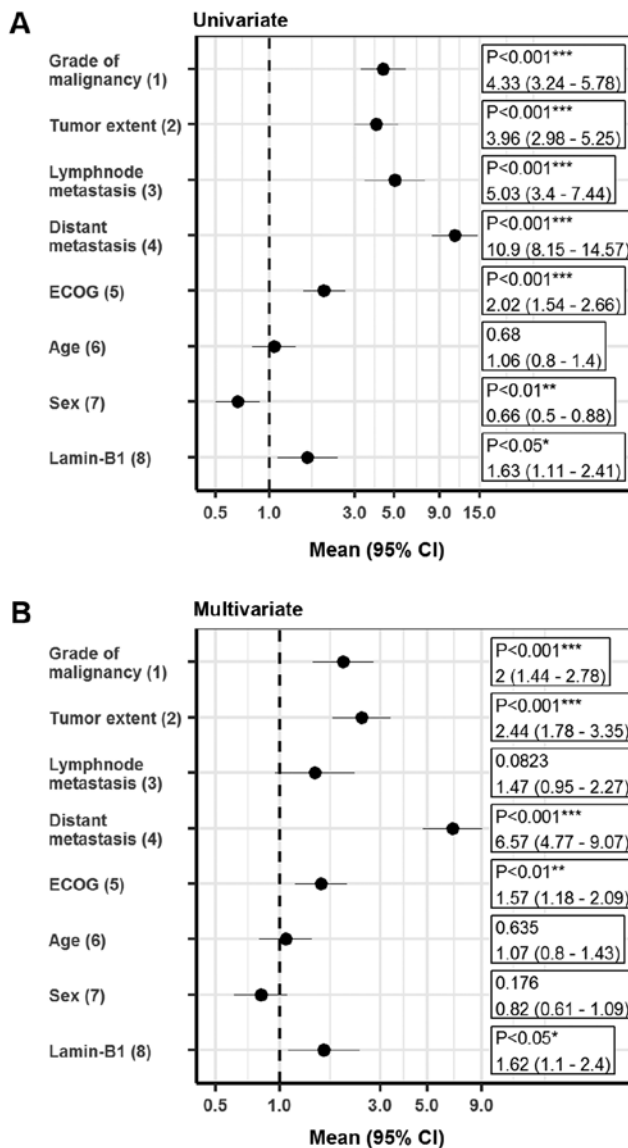
Figure 4. Survival analysis. (A) Univariate and (B) multivariate survival analysis of prognostic factors influencing cancer-specific survival in clear cell renal cell carcinomas represented as forest plots, where the following comparisons have been applied: (1) G3 vs. G1/G2; (2) pT3/pT4 vs. pT1/pT2; (3) pN1/pN2 vs. N0/pN0; (4) M1 vs. M0; (5) ≥1 vs. 0; (6) >65 vs. ≤65%; (7) female vs. male; and (8) >60 % vs. ≤60%. *P<0.05, **P<0.01 and ***P<0.001. ECOG, Eastern Cooperative Oncology Group; CI, confidence interval.

hazards model. Notably, LMNB1 expression qualified as an independent prognostic marker for cancer-specific survival after adjustments for established prognostic factors (grade of malignancy, tumor extent, lymph node metastasis, distant metastasis, ECOG performance status and gender) in the multiple regression analysis for ccRCC patients (HR, 1.62; 95% CI, 1.1-2.4; Fig. 4). After adjustment for prognostic factors, LMNB1 expression also remained statistically significant for patients with localized disease (HR, 1.82; 95% CI, 1.09-3.02; Fig. S1).

To further elucidate the relationship between LMNB1 expression and patient prognosis, the present study utilized TCGA data on ccRCC. When tumors were grouped according to LMNB1 mRNA levels (a Z-score >1.96 indicated upregulation and a Z-Score ≤1.96 and >-1.96 indicated no

regulation when considering that a Z-score of 1.96 presents the approximate value of the 97.5 percentile point of the normal distribution; 95% of the area under a normal curve lies within roughly 1.96 standard deviations of the mean), univariate survival analysis revealed that 77 out of 176 patients (43.75%) with increased LMNB1 mRNA levels were deceased whereas only 83 out of 357 (23.25%) of the patients without elevated mRNA levels were deceased (P≤0.0001); the Kaplan-Meier curves are depicted in Fig. S2.

LMNB1 is regulated during etoposide-induced senescence. LMNB1 downregulation is known as a senescence effector (15). To investigate whether the downregulation of LMNB1 plays a role in cellular senescence in RCC the present study conducted *in-vitro* studies. A total of 4 different RCC cell lines (ACHN, Caki-2, 786-O and 769-P) were subjected to etoposide-induced senescence as described by Nagano *et al* (30). As expected, treatment reduced the proliferation rate; however, the effects varied widely between the different cell lines. Notably, a strong reduction in LMNB1 expression was accompanied by a stronger decrease in proliferation in 3 of the 4 cell lines (Caki-2, 786-O and 769-P), and the cell line ACHN, with the lowest effects on LMNB1 expression, also exhibited a reduced effect of etoposide treatment on the proliferation rate (Fig. 5). ACHN, 786-O and 769-P are ccRCC cell lines. Caki-2 was originally defined as a ccRCC cell line, however, a growing body of evidence has suggested that this cell line may actually be papillary RCC (31,32). This suggests that LMNB1 is functional not only in ccRCC but also in other subtypes of RCC.

Discussion

RCCs are known to be resistant to conventional radio- and chemotherapy, therefore, traditional immunotherapy, such as high-dose interleukin-2 and interferon-α, has been the standard treatment in patients with systemic disease in the past. Currently, targeted antiangiogenic therapies and novel immunotherapy agents, such as checkpoint inhibitors, have become an integral part of the management of metastatic RCC (33). However, the development of resistance often occurs and the chance of recovery is marginal. Therefore, new therapeutic targets are urgently needed to develop novel drugs with different mechanisms of action (34).

The results of the present study have revealed a high LMNB1 expression in 80% of the analyzed ccRCC tumors, without pre-selecting for a specific tumor or patients parameter. LMNB1 is a senescence effector and triggers widespread changes in gene expression upon down regulation (15). In agreement with this biological function, the present study identified high LMNB1 expression as an unfavorable prognostic marker in ccRCC patients. This indicated that the *VHL* loss-induced senescence program (4) may be bypassed in RCC development by a currently unknown mechanism, resulting in continuous LMNB1 expression. However, *in vitro* experiments demonstrated that etoposide-induced senescence may be associated with LMNB1 reduction in ccRCC and papillary RCC cell lines. Notably, it appears that there is a link between LMNB1 expression and the cell proliferation rate (5).
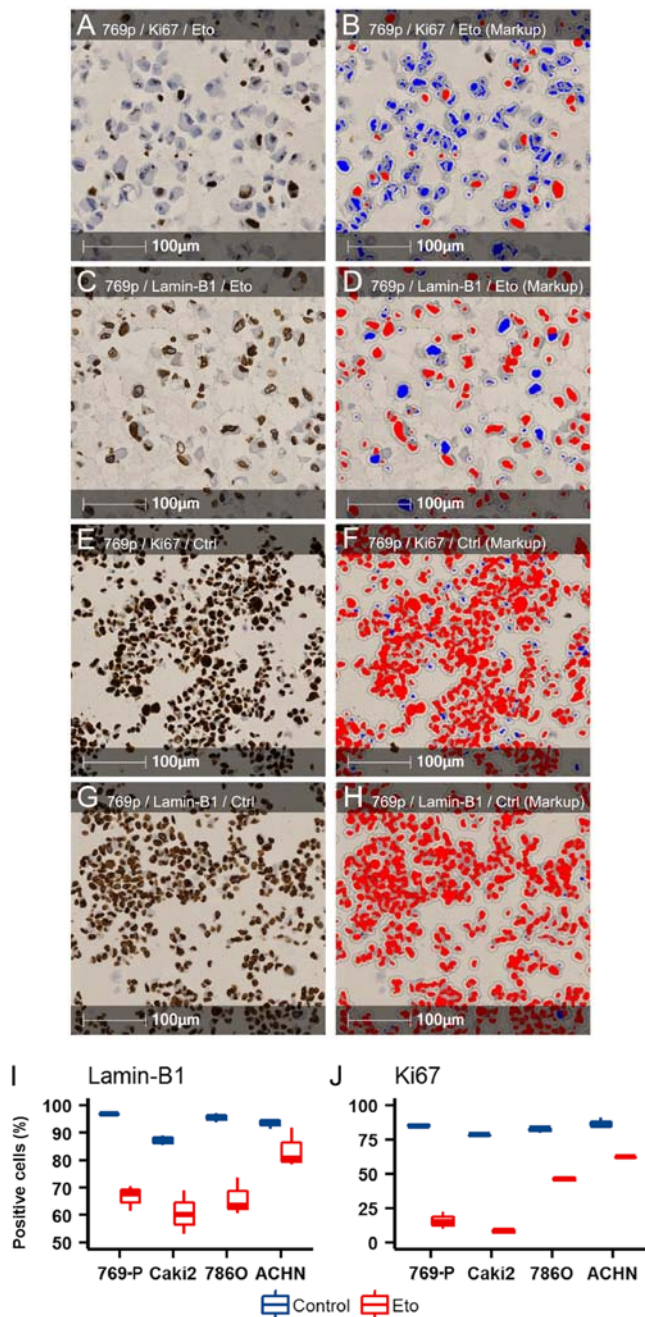
Figure 5. Regulation of Lamin-B1 in RCC cell lines upon etoposide treatment. Representative (A and E) Ki-67 and (C and G) Lamin-B1 staining of (A and C) etoposide treated and (E and G) untreated 769-P cells. (B, D, F and H) Corresponding positive cell count markup. Blue indicates negative nuclei; and red indicates positive nuclei. (I and J) Box plots demonstrating the differences in the etoposide response in RCC cell lines. RCC, renal cell carcinoma; Eto, etoposide; Ctrl, control.

cyclin-dependent kinase inhibitors have proven effective by invoking a senescence response (36). Zhu *et al* (37) reported that the tyrosine kinase inhibitor sunitinib used as a first-line therapeutic agent against metastatic RCC induced cellular senescence in renal cell carcinoma cells and exhibited similar effects *in vivo* following xenograft experiments in nude mice. In addition, immunohistochemical studies demonstrated a senescence-phenotype in tumor tissues from patients with RCC after neoadjuvant sunitinib treatment (37). Thus, reinforcing a therapy-induced senescence therapy by adding a novel synthetic compound such as STK899704, which suppresses the proliferation of a broad range of cancer cell types, may offer a novel therapeutic strategy for patients with advanced RCC (38).

Availability of data and materials

The datasets generated and/or analyzed during the current study are available from the corresponding author on reasonable request.

Authors' contributions

MMR, MS, PS, SF, KET and SMG conceived and designed the experiments. EH, MH, GH and WR obtained the patients' data and the corresponding tissue specimens. MMR, MS and SMG wrote the manuscript with input from all authors. All authors discussed the results and contributed to the final manuscript.

Ethics approval and consent to participate

The human tissue samples were provided by the Tissue Bank of the National Centre for Tumor Diseases Heidelberg (Heidelberg, Germany) and used retrospectively with approval from the Ethics Committee of the University of Heidelberg (Heidelberg, Germany).

Patient consent for publication

Not applicable.

Competing interests

The authors declare that they have no competing interests.

RCCs with high LMNB1 expression predominantly exhibited higher proliferation rates when compared with those with low LMNB1 expression (Fig. S3). This indicated that LMNB1 may be a functional downstream senescence effector in RCC and may serve as a potential predictive biomarker for innovative senescence-based therapeutic approaches in ccRCC.

Therapy-induced senescence represents a novel functional target that may improve cancer therapy (35). In recent years, therapeutic approaches such as p53 reactivation, inhibition of c-MYC in p53- or c-MYC-driven tumors, or treatment with

References

1. Moch H, Humphrey PA, Ulbright T and Reuter V (eds): WHO Classification of Tumours of the Urinary System and Male Genital Organs. 4th edition. IARC, Lyon, 2016.
2. Jonasch E, Futreal PA, Davis IJ, Bailey ST, Kim WY, Brugarolas J, Giaccia AJ, Kurban G, Pause A, Frydman J, et al: State of the science: An update on renal cell carcinoma. Mol Cancer Res 10: 859-880, 2012.
3. Kaelin WG Jr: The von Hippel-Lindau tumour suppressor protein: O2 sensing and cancer. Nat Rev Cancer 8: 865-873, 2008.
4. Young AP, Schlisio S, Minamishima YA, Zhang Q, Li L, Grisanzio C, Signoretti S and Kaelin WG Jr: VHL loss actuates a HIF-independent senescence programme mediated by Rb and p400. Nat Cell Biol 10: 361-369, 2008.
5. Macher-Goeppinger S, Bermejo JL, Schirmacher P, Pahernik S, Hohenfellner M and Roth W: Senescence-associated protein p400 is a prognostic marker in renal cell carcinoma. Oncol Rep 30: 2245-2253, 2013.
6. Welford SM, Dorie MJ, Li X, Haase VH and Giaccia AJ: Renal oxygenation suppresses VHL loss-induced senescence that is caused by increased sensitivity to oxidative stress. Mol Cell Biol 30: 4595-4603, 2010.
7. Courtois-Cox S, Genther Williams SM, Reczek EE, Johnson BW, McGillicuddy LT, Johannessen CM, Hollstein PE, MacCollin M and Cichowski K: A negative feedback signaling network underlies oncogene-induced senescence. Cancer Cell 10: 459-472, 2006.
8. Michaloglou C, Vredeveld LC, Soengas MS, Denoyelle C, Kuilman T, van der Horst CM, Majoor DM, Shay JW, Mooi WJ and Peeper DS: BRAFE600-associated senescence-like cell cycle arrest of human naevi. Nature 436: 720-724, 2005.
9. Chen Z, Trotman LC, Shaffer D, Lin HK, Dotan ZA, Niki M, Koutcher JA, Scher HI, Ludwig T, Gerald W, et al: Crucial role of p53-dependent cellular senescence in suppression of Pten-deficient tumorigenesis. Nature 436: 725-730, 2005.
10. Serrano M, Lin AW, McCurrach ME, Beach D and Lowe SW: Oncogenic ras provokes premature cell senescence associated with accumulation of p53 and p16INK4a. Cell 88: 593-602, 1997.
11. Kuilman T, Michaloglou C, Mooi WJ and Peeper DS: The essence of senescence. Genes Dev 24: 2463-2479, 2010.
12. Shimi T, Butin-Israeli V, Adam SA, Hamanaka RB, Goldman AE, Lucas CA, Shumaker DK, Kosak ST, Chandel NS and Goldman RD: The role of nuclear lamin B1 in cell proliferation and senescence. Genes Dev 25: 2579-2593, 2011.
13. Jung HJ, Lee JM, Yang SH, Young SG and Fong LG: Nuclear lamins in the brain-new insights into function and regulation. Mol Neurobiol 47: 290-301, 2013.
14. Hallstrom TC, Mori S and Nevins JR: An E2F1-dependent gene expression program that determines the balance between proliferation and cell death. Cancer Cell 11: 11-22, 2008.
15. Shah PP, Donahue G, Otte GL, Capell BC, Nelson DM, Cao K, Aggarwala V, Cruickshanks HA, Rai TS, McBryan T, et al: Lamin B1 depletion in senescent cells triggers large-scale changes in gene expression and the chromatin landscape. Genes Dev 27: 1787-1799, 2013.
16. Padiath QS, Saigoh K, Schiffmann R, Asahara H, Yamada T, Koeppen A, Hogan K, Ptácek LJ and Fu YH: Lamin B1 duplications cause autosomal dominant leukodystrophy. Nat Genet 38: 1114-1123, 2006.
17. Moss SF, Krivosheyev V, de Souza A, Chin K, Gaetz HP, Chaudhary N, Worman HJ and Holt PR: Decreased and aberrant nuclear lamin expression in gastrointestinal tract neoplasms. Gut 45: 723-729, 1999.
18. Broers JL, Raymond Y, Rot MK, Kuijpers H, Wagenaar SS and Ramaekers FC: Nuclear A-type lamins are differentially expressed in human lung cancer subtypes. Am J Pathol 143: 211-220, 1993.
19. Coradeghini R, Barboro P, Rubagotti A, Boccardo F, Parodi S, Carmignani G, D'Arrigo C, Patrone E and Balbi C: Differential expression of nuclear lamins in normal and cancerous prostate tissues. Oncol Rep 15: 609-613, 2006.
20. Sun S, Xu MZ, Poon RT, Day PJ and Luk JM: Circulating Lamin B1 (LMNB1) biomarker detects early stages of liver cancer in patients. J Proteome Res 9: 70-78, 2010.
21. Izdebska M, Gagat M and Grzanka A: Overexpression of lamin B1 induces mitotic catastrophe in colon cancer LoVo cells and is associated with worse clinical outcomes. Int J Oncol 52: 89-102, 2018.
22. Li L, Du Y, Kong X, Li Z, Jia Z, Cui J, Gao J, Wang G and Xie K: Lamin B1 is a novel therapeutic target of betulinic acid in pancreatic cancer. Clin Cancer Res 19: 4651-4661, 2013.
23. Macher-Goeppinger S, Aulmann S, Tagscherer KE, Wagener N, Haferkamp A, Penzel R, Brauckhoff A, Hohenfellner M, Sykora J, Walczak H, et al: Prognostic value of tumor necrosis factor-related apoptosis-inducing ligand (TRAIL) and TRAIL receptors in renal cell cancer. Clin Cancer Res 15: 650-659, 2009.
24. Gringon D, Eble J, Bonsib SM and Moch H: Pathology and Genetics of Tumors of the Urinary System & Male Genital Organs. eds. Eble JN, Sauter G, Epstein J, Sesterhenn I. Clear cell renal cell carcinoma. IARC: Lyon, France: 23-25, 2004.
25. Sobin L, Gospodarowicz M and Wittekind C: TNM Classification of Malignant Tumours, 7th Edition, 2009.
26. Foersch S, Schindeldecker M, Keith M, Tagscherer KE, Fernandez A, Stenzel PJ, Pahernik S, Hohenfellner M, Schirmacher P, Roth W and Macher-Goeppinger S: Prognostic relevance of androgen receptor expression in renal cell carcinomas. Oncotarget 8: 78545-78555, 2017.
27. Budczies J, Klauschen F, Sinn BV, Győrffy B, Schmitt WD, Darb-Esfahani S and Denkert C: Cutoff Finder: A comprehensive and straightforward Web application enabling rapid biomarker cutoff optimization. PLoS One 7: e51862, 2012.
28. Shvarts O, Lam JS, Kim HL, Han KR, Figlin R and Belldegrun A: Eastern Cooperative Oncology Group performance status predicts bone metastasis in patients presenting with renal cell carcinoma: Implication for preoperative bone scans. J Urol 172: 867-870, 2004.
29. Hertz-Picciotto I and Rockhill B: Validity and efficiency of approximation methods for tied survival times in Cox regression. Biometrics 53: 1151-1156, 1997.
30. Nagano T, Nakano M, Nakashima A, Onishi K, Yamao S, Enari M, Kikkawa U and Kamada S: Identification of cellular senescence-specific genes by comparative transcriptomics. Sci Rep 6: 31758, 2016.
31. Brodaczewska KK, Szczylik C, Fiedorowicz M, Porta C and Czarnecka AM: Choosing the right cell line for renal cell cancer research. Mol Cancer 15: 83, 2016.
32. Furge KA, Chen J, Koeman J, Swiatek P, Dykema K, Lucin K, Kahnoski R, Yang XJ and Bin TT: Detection of DNA copy number changes and oncogenic signaling abnormalities from gene expression data reveals MYC activation in high-grade papillary renal cell carcinoma. Can Res 67: 3171-3176, 2007.
33. Barata PC and Rini BI: Treatment of renal cell carcinoma: Current status and future directions. CA Cancer J Clin 67: 507-524, 2017.
34. Choueiri TK and Motzer RJ: Systemic therapy for metastatic renal-cell carcinoma. N Engl J Med 376: 354-366, 2017.
35. Ewald JA, Desotelle JA, Wilding G and Jarrard DF: Therapy-induced senescence in cancer. J Natl Cancer Inst 102: 1536-1546, 2010.
36. Acosta JC and Gil J: Senescence: A new weapon for cancer therapy. Trends Cell Biol 22: 211-219, 2012.
37. Zhu Y, Xu L, Zhang J, Hu X, Liu Y, Yin H, Lv T, Zhang H, Liu L, An H, et al: Sunitinib induces cellular senescence via p53/Dec1 activation in renal cell carcinoma cells. Cancer Sci 104: 1052-1061, 2013.
38. Park CW, Bak Y, Kim MJ, Srinivasrao G, Hwang J, Sung NK, Kim BY, Yu JH, Hong JT and Yoon DY: The novel small molecule STK899704 promotes senescence of the human A549 NSCLC cells by inducing DNA damage responses and cell cycle arrest. Front Pharmacol 9: 163, 2018.